J|A|C|S COMMUNICATIONS

Published on Web 12/29/2008

ZnO-Templated Synthesis of Wurtzite-Type ZnS and ZnSe Nanoparticles

Farah Dawood and Raymond E. Schaak*

Department of Chemistry and Materials Research Institute, The Pennsylvania State University, University Park, Pennsylvania 16802

Received October 28, 2008; E-mail: schaak@chem.psu.edu

Wide bandgap semiconductor nanocrystals have attracted significant attention in the past few years because of their size-dependent properties and diverse applications.[1−3] In particular, ZnS is an important phosphor host material[4] and, when appropriately doped, can exhibit luminescent properties.[5] Likewise, ZnSe has applications in light emitting diodes and photodetectors.[6] While ZnS and ZnSe crystallize in both the zincblende (ZB) and wurtzite (WZ) structures, ZB is the most stable. The WZ polymorphs, which are often desired because of their wider bandgaps and improved luminescence properties,[7] are metastable. While several examples of WZ-type ZnS and ZnSe nanocrystals have been reported using techniques that include precursor decomposition via solvothermal reactions,[8] ultrasonication,[9] and colloidal methods,[10] the ZB structure is predominant. Because of the subtle structural differences between the ZB and WZ structures, subtle synthetic differences can favor one polymorph over the other. Consequently, it remains challenging to predictably generate the WZ polymorphs and understand the factors that play a key role in their formation.

Here we show that ZnO nanoparticles, which adopt the WZ structure, can serve as structural templates for the controllable formation of WZ-type ZnS and ZnSe. This finding is the result of detailed mechanistic studies involving methods known to produce WZ-type ZnS. The results point to the importance of forming WZ-type ZnO as a reaction intermediate in order to preferentially stabilize the WZ forms of ZnS and ZnSe.

WZ-type ZnS was initially synthesized using a modification of a procedure reported by Zhao et al.[10a] Briefly, $ZnCl_2$ (0.298 g) and tetramethylammonium hydroxide (TMAH, 0.794 g) were dissolved in 15 mL of ethylene glycol (EG) and heated to 100 °C. An EG solution of thiourea (0.167 g in 15 mL) was then added and the reaction was further heated to 160 °C, with aliquots taken every 10 °C from 100−160 °C to probe the reaction pathway.

Figure 1a shows powder X-ray diffraction (XRD) data for a typical WZ-type ZnS nanoparticle product. Figure 1b shows XRD data for the aliquots taken during the reaction. At 100 °C, the product is nanocrystalline ZnO, indicating that ZnO forms initially prior to ZnS. This is reasonable when considering the chemistry: ZnO nanoparticles are known to precipitate within minutes when Zn^{2+} is reacted with TMAH in EG in this temperature range.[11] As the reaction progresses, the ZnO gradually transforms into WZ-type ZnS, converting completely to ZnS by 160 °C. Quantitative analysis of the XRD data for the final ZnS product (160 °C sample) indicates that a majority of the sample (70%) consists of the WZ polymorph.

Transmission electron microscope (TEM) images show the ZnO nanoparticles formed in situ during the reaction that generates WZ-type ZnS (Figure 2a), as well as the WZ-type product (Figure 2b). Both appear morphologically similar: the primary particle sizes are 5−7 nm, and they aggregate to form ∼100 nm agglomerates. Scherrer analysis indicates particle sizes of 4−7 nm, which is consistent with the TEM data. Photoluminescence (PL) data (Figure 2c) further confirms the presence of the ZnO intermediate and the WZ-type ZnS product. The emission peaks in the PL spectra of ZnO (∼360 nm) and ZnS (∼330 nm) are consistent with previously reported values.[12]

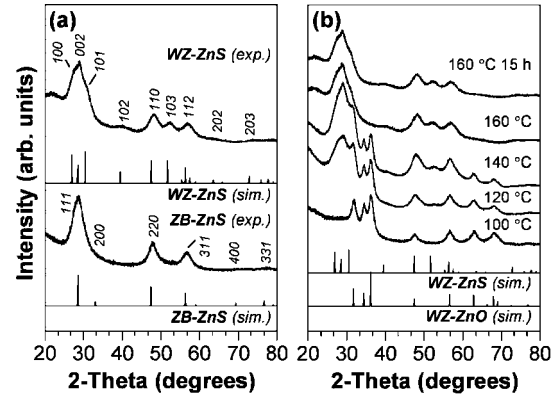

Figure 1. Powder XRD data for (a) WZ-ZnS (ZnO intermediate) and ZB-ZnS (no ZnO intermediate) and (b) samples isolated from aliquots taken during the formation of WZ-ZnS, showing a progression from WZ-ZnO to WZ-ZnS. Simulated XRD data are shown for comparison.

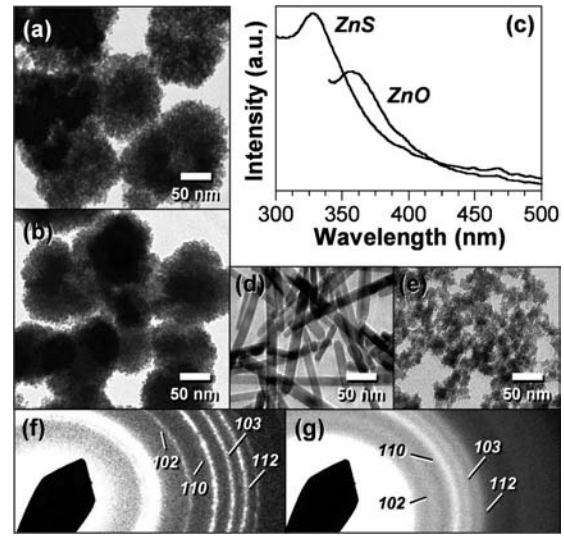

Figure 2. TEM images of (a) ZnO intermediate and (b) WZ-ZnS product; (c) room-temperature PL data for ZnO and WZ-ZnS; TEM images of (d) ZnO nanorod precursor and (e) WZ-ZnS nanoparticle product; SAED patterns for (f) ZnO from panel d and (g) WZ-ZnS from panel e.

In a control experiment designed to produce ZnS using an analogous procedure but under conditions that do not first nucleate ZnO, ZB-type ZnS forms exclusively (Figure 1a). Specifically, substituting ethylenediamine (en) for TMAH and adding thiourea at 100 °C as before, with all other conditions identical, does not generate a ZnO intermediate. Heating ZB-ZnS leads only to further

10.1021/ja808455u CCC: $40.75

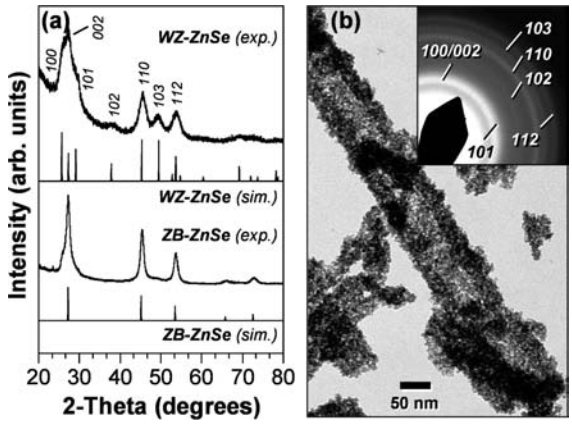

Figure 3. (a) Powder XRD data for WZ-ZnSe (ZnO intermediate) and ZB-ZnSe (no ZnO intermediate). (b) TEM image of an assembly of WZ-ZnSe nanoparticles. Inset: SAED pattern for WZ-ZnSe nanoparticles.

crystallization and growth of that phase, not transformation into WZ-ZnS. This implies that the WZ structure of the ZnO intermediate may help to template the formation of WZ-type ZnS, since without the ZnO intermediate but with otherwise identical conditions, the ZB polymorph forms.

Further support for the proposed mechanism comes from applying the in situ observations to a deliberately designed ex-situ system: the conversion of preformed ZnO nanoparticles into WZ-type ZnS. ZnO nanorods[13] (see Supporting Information for details) were added to EG and reacted with thiourea. Figure 2d shows a TEM image of the ZnO nanorods, which have diameters of approximately 10 nm. Figure 2e shows a TEM image of the product. Selected area electron diffraction (SAED) patterns confirm the WZ structure of both ZnO and ZnS (Figure 2f,g). The WZ-ZnS product does not retain the nanorod morphology. However, the particle diameters are around 10 nm, which is consistent with the ZnO nanorod breaking apart along its length during the chemical transformation while maintaining its overall limiting size. This hints at the atomic-scale mechanism, which may involve an ion exchange pathway that nominally replaces oxygen with sulfur. Such a pathway would help preserve the framework because of the low reaction temperatures and high reactivity of the nanoscale solid but disrupt and fracture the structure because of the significant size difference between oxygen and sulfur.

Another control experiment provides further support for the proposed mechanism. Preformed ZnO nanoparticles react with thiourea in EG to form WZ-ZnS. However, the same ZnO nanoparticles react with thiourea in water, under otherwise identical conditions, to form ZB-ZnS. Under the basic reaction conditions (pH 9), ZnO nanoparticles dissolve and therefore are not present as a structural template, resulting in the precipitation of ZB-ZnS. In EG under these conditions, ZnO is not soluble, allowing it to serve as a structural template to form WZ-ZnS.

This structure-templating mechanism can be applied to ZnSe, which also typically forms ZB-type nanocrystals. XRD data (Figure 3a) confirms that WZ-ZnSe is selectively formed under conditions where ZnO forms as a reaction intermediate, while ZB-ZnSe forms when no ZnO intermediate is present. SAED confirms that the nanoparticle products are WZ-type ZnSe, clearly showing the *102* and *103* reflections that differentiate the WZ and ZB polymorphs. The WZ-ZnSe nanocrystals tend to assemble into aggregates such as the one-dimensional array shown in Figure 3b. This phenomenon can be rationalized by the known permanent dipole moment of ZnSe and other WZ-type semiconductor nanocrystals and is similar to results obtained for PbSe and related nanocrystal systems.[14]

By studying the reaction pathway involved in the formation of WZ-ZnS nanoparticles, we discovered that WZ-ZnO forms first as a reaction intermediate. This provides a predictable pathway for generating WZ-type ZnS and ZnSe nanoparticles, and may also help to rationalize previous reports where the WZ-type structures were formed rather than the more stable ZB polymorphs. It should be possible to expand this chemistry to other systems where metastable polymorphs are desired, as well as apply conditions that favor morphological retention in order to rigorously tune nanocrystal size and shape and study the size dependence of the transformation.

Acknowledgment. This work was supported by NSF (DMR-0748943), the Petroleum Research Fund (administered by the American Chemical Society), a Beckman Young Investigator Award, a Sloan Research Fellowship, a DuPont Young Professor Grant, and a Camille Dreyfus Teacher-Scholar Award. TEM was performed at the Huck Institutes of the Life Sciences. The authors thank Carl Myers and Prof. Mary Beth Williams for help with collecting the photoluminescence data.

Supporting Information Available: Experimental details, additional XRD data, and SAED patterns. This material is available free of charge via the Internet at http://pubs.acs.org.

References

(1) Alivisatos, A. P. *Science* **1996**, *271*, 933–937.
(2) Fang, X.; Bando, Y.; Gautam, U. K.; Ye, C.; Goldberg, D. *J. Mater. Chem.* **2008**, *18*, 509–522.
(3) Medintz, I. L.; Uyeda, H. T.; Goldman, E. R.; Mattoussi, H. *Nat. Mater.* **2005**, *4*, 435–446.
(4) Monroy, E.; Omnes, F.; Calle, F. *Semicond. Sci. Technol.* **2003**, *18*, R33–R51.
(5) (a) Bhargava, R. N.; Gallagher, D.; Hong, X.; Nurmikko, D. *Phys. Rev. Lett.* **1994**, *72*, 416–419. (b) Sooklal, K.; Cullum, B. S.; Angel, S. M.; Murphy, C. J. *J. Phys. Chem.* **1996**, *100*, 4551–4555.
(6) (a) Jeon, H.; Ding, J.; Patterson, W.; Nurmikko, A. V.; Xie, W.; Grillo, D. C.; Kobayashi, M.; Gunshor, R. L. *Appl. Phys. Lett.* **1991**, *59*, 3619–3621. (b) Wang, J.; Hutchins, D. C.; Miller, A.; Van Stryland, E. W.; Welford, K. R.; Muirhead, I. T.; Lewis, K. L. *J. Appl. Phys.* **1993**, *73*, 4746–4751.
(7) (a) Qadri, S. B.; Skelton, E. F.; Dinsmore, A. D.; Hu, J. Z.; Kim, W. J.; Nelson, C.; Ratna, B. R. *J. Appl. Phys.* **2001**, *89*, 115–119. (b) Wang, Z.; Daemen, L. L.; Zhao, Y.; Zha, C. S.; Downs, R. T.; Wang, X.; Wang, Z. L.; Hemley, R. J. *Nat. Mater.* **2005**, *4*, 922–927.
(8) (a) Yu, S. H.; Yoshimura, M. *Adv. Mater.* **2002**, *14*, 296–300. (b) Deng, Z. X.; Wang, C.; Sun, X. M.; Li, Y. D. *Inorg. Chem.* **2002**, *41*, 869–873.
(9) Geng, J.; Liu, B.; Xu, L.; Hu, F. N.; Zhu, J. J. *Langmuir* **2007**, *23*, 10286–10293.
(10) (a) Zhao, Y.; Zhang, Y.; Zhu, H.; Hadjipanayis, G. C.; Xiao, J. Q. *J. Am. Chem. Soc.* **2004**, *126*, 6874–6875. (b) Cozzoli, P. D.; Manna, L.; Curri, M. L.; Kudera, S.; Giannini, C.; Striccoli, M.; Agostiano, A. *Chem. Mater.* **2005**, *17*, 1296–1306. (c) Panda, A. B.; Acharya, S.; Efrima, S.; Golan, Y. *Langmuir* **2007**, *23*, 765–770.
(11) Wang, M.; Na, E. K.; Kim, J. S.; Kim, E. J.; Hahn, S. H.; Park, C.; Koo, K. K. *Mater. Lett.* **2007**, *61*, 4094.
(12) (a) Du, X. W.; Fu, Y. S.; Sun, J.; Han, X.; Liu, J. *Semicond. Sci. Technol.* **2006**, *21*, 1202–1206. (b) Cheng, C.; Xu, G.; Zhang, H.; Cao, J.; Jiao, P.; Wang, X. *Mater. Lett.* **2006**, *60*, 3561–3564. (c) Irimpan, L.; Nampoori, V. P. N.; Radhakrishnan, P.; Deepthy, A.; Krishnan, B. *J. Appl. Phys.* **2007**, *102*, 063524-1–063524-6.
(13) (a) Wang, C.; Shen, E.; Wang, E.; Gao, L.; Kang, Z.; Tian, C.; Lan, Y.; Zhang, C. *Mater. Lett.* **2005**, *59*, 2867–2871. (b) Cheng, B.; Shi, W.; Russell-Tanner, J. M.; Zhang, L.; Samulski, E. T. *Inorg. Chem.* **2006**, *45*, 1208–1214.
(14) (a) Shim, M.; Guyot-Sionnest, P. *J. Chem. Phys.* **1999**, *111*, 6955–6964. (b) Cho, K. S.; Talapin, D. V.; Gaschler, W.; Murray, C. B. *J. Am. Chem. Soc.* **2005**, *127*, 7140–7147.

JA808455U